



UNIVERSITY OF LEEDS

This is a repository copy of *A neural network approach for determining gait modifications to reduce the contact force in knee joint implant.*

White Rose Research Online URL for this paper:  
<http://eprints.whiterose.ac.uk/92192/>

Version: Accepted Version

---

**Article:**

Ardestani, MM, Chen, Z, Wang, L et al. (5 more authors) (2014) A neural network approach for determining gait modifications to reduce the contact force in knee joint implant. *Medical Engineering and Physics*, 36 (10). pp. 1253-1265. ISSN 1350-4533

<https://doi.org/10.1016/j.medengphy.2014.06.016>

---

© IPEM. Published by Elsevier Ltd.. Licensed under the Creative Commons Attribution-NonCommercial-NoDerivatives 4.0 International  
<http://creativecommons.org/licenses/by-nc-nd/4.0/>

**Reuse**

Unless indicated otherwise, fulltext items are protected by copyright with all rights reserved. The copyright exception in section 29 of the Copyright, Designs and Patents Act 1988 allows the making of a single copy solely for the purpose of non-commercial research or private study within the limits of fair dealing. The publisher or other rights-holder may allow further reproduction and re-use of this version - refer to the White Rose Research Online record for this item. Where records identify the publisher as the copyright holder, users can verify any specific terms of use on the publisher's website.

**Takedown**

If you consider content in White Rose Research Online to be in breach of UK law, please notify us by emailing [eprints@whiterose.ac.uk](mailto:eprints@whiterose.ac.uk) including the URL of the record and the reason for the withdrawal request.



[eprints@whiterose.ac.uk](mailto:eprints@whiterose.ac.uk)  
<https://eprints.whiterose.ac.uk/>

# A Neural Network Approach for Determining Gait Modifications to Reduce the Contact Force in Knee Joint Implant

Marzieh Mostafavizadeh Ardestani<sup>1</sup>, Zhenxian Chen<sup>1</sup>, Ling Wang<sup>1\*</sup>, Qin Lian<sup>1</sup>, Yaxiong Liu<sup>1</sup>, Jiankang He<sup>1</sup>,  
Dichen Li<sup>1</sup> and Zhongmin Jin<sup>1,2</sup>

<sup>1</sup>State Key Laboratory for Manufacturing Systems Engineering, *School of Mechanical Engineering, Xi'an Jiaotong University, 710049, Xi'an, Shaanxi, China*

<sup>2</sup>Institute of Medical and Biological Engineering, School of Mechanical Engineering, University of Leeds, Leeds, LS2 9JT, UK

\* Corresponding author Tel.: +0-86-029-83395187; E-mail: menlwang@mail.xjtu.edu.cn

## Abstract

There is a growing interest in non-surgical gait rehabilitation treatments to reduce the loading in the knee joint. In particular, synergetic kinematic changes required for joint offloading should be determined individually for each subject. Previous studies for gait rehabilitation designs are typically relied on a “trial-and-error” approach, using multi-body dynamic (MBD) analysis. However MBD is fairly time demanding which prevents it to be used iteratively for each subject.

This study employed an artificial neural network to develop a cost-effective computational framework for designing gait rehabilitation patterns. A feed forward artificial neural network (FFANN) was trained based on a number of experimental gait trials obtained from literature. The trained network was then hired to calculate the appropriate kinematic waveforms (output) needed to achieve desired knee joint loading patterns (input). An auxiliary neural network was also developed to update the ground reaction force and moment profiles with respect to the predicted kinematic waveforms. The feasibility and efficiency of the predicted kinematic patterns were then evaluated through MBD analysis.

Results showed that FFANN-based predicted kinematics could effectively decrease the total knee joint reaction forces. Peak values of the resultant knee joint forces, with respect to the bodyweight (BW), were reduced by 20%BW and 25%BW in the midstance and the terminal stance phases. Impulse values of the knee joint loading patterns were also decreased by 17%BW\*s and 24%BW\*s in the corresponding phases. The FFANN-based framework suggested a cost-effective forward solution which directly calculated the kinematic variations needed to implement a given desired knee joint loading pattern. It is therefore expected that this approach provides potential advantages and further insights into knee rehabilitation designs.

**Keywords:** Gait modification, kinematics, knee joint loading, neural network, multi-body dynamics

## 1 Introduction

2 Non-invasive gait rehabilitation strategies are of significant advantages for patients with knee  
3 osteoarthritis (OA). Pre-surgical gait rehabilitation can decrease pain, decelerate joint disease progression  
4 and post-pone surgery[1, 2]. Post-surgical gait rehabilitation can also accelerate patient recovery[3, 4],  
5 reinforce joint functionality[5, 6], decrease gait asymmetry[7] and augment the durability and longevity of  
6 the implanted prostheses[8, 9]. Gait rehabilitation mainly aims to decrease knee joint loading through minor  
7 changes in human gait patterns. Recognizing the synergistic kinematic changes, required for joint  
8 offloading, however has been a very challenging task. Although various gait modifications have been  
9 developed in association with knee joint offloading [10-22], none of them have yet been accepted as a  
10 general modification strategy. In fact, large inter-patient variability has been reported in gait kinematics and  
11 joint loading patterns[23, 24] which may directly affect the results and the efficiency of gait rehabilitation  
12 from one group of patients to another group. In other words, a gait rehabilitation might be effective for joint  
13 offloading in a group of participants [13, 16, 25] while it might be ineffective[26] or even detrimental [27]  
14 for other groups of patients. Thus, gait rehabilitation strategies should be determined individually for each  
15 subject.

16 Current studies for gait rehabilitation design have been typically carried out based on multi-body  
17 dynamics (MBD) analysis[13, 14]. Although MBD can determine the knee joint loadings from known gait  
18 kinematics, the nonlinear relationship between kinematic variations and knee joint offloading is still  
19 unknown. Available techniques therefore, require iterative “trial-and-error” attempts of MBD analysis to  
20 recognize the most influential kinematic variations needed for joint offloading. In each attempt, kinematic  
21 waveforms and ground reaction forces (GRFs) should be collected experimentally or produced  
22 computationally and then imported into an inverse dynamic analysis to calculate the resultant joint  
23 moments. MBD computations should be repeated until a reasonable reduction in knee joint loading is  
24 achieved. This “trial-and-error” approach of MBD would be fairly time demanding and prevent this method  
25 to be used iteratively for each subject. Thus, a cost-effective surrogate model which replicates the original  
26 MBD would be of much advantage.

27 Furthermore, previous studies have been mainly performed to reduce knee adduction moment (KAM)  
28 as a surrogate of medial knee contact force (KCF) [28] but KAM is not always a reliable measure for knee  
29 joint offloading: (1) gait modifications that reduce KAM are not guaranteed to reduce KCF[29]; (2)  
30 interpreting the KAM is highly dependent on the chosen reference frame (e.g., laboratory, tibia, femur and

31 floating reference frames). This reference dependency can potentially yield to inconsistent results from one  
32 laboratory to another [16, 26]. Accordingly, gait modification strategies should directly aim to decrease  
33 KCF.

34 Artificial neural network (ANN) has been commonly used in various fields of biomechanics as a cost-  
35 effective surrogate model [30-33]. Once a set of inputs and resultant outputs are presented to the network,  
36 ANN learns the causal interactions between input and output variables. Given a new set of inputs, the  
37 trained neural network (surrogate model) can generalize the relationship to produce the associated outputs.  
38 Therefore it releases the necessity of running the original physics-based model or repeating the time-  
39 consuming iterations [34]. In human gait studies, ANN has been particularly used as an alternative to MBD  
40 analysis to investigate joint moments [35-38], gait kinematics [39] and ground reaction forces [40-42]. It is  
41 therefore expected that ANN can also provide further insight into the interactions between gait kinematics  
42 and resultant knee joint loads.

43 Although ANN has been used to calculate knee joint loadings from gait kinematics [43], it has not been  
44 used to solve the inverse problem. The underlying hypothesis of this study was that ANN can be used to  
45 calculate gait kinematics for a given joint loading pattern. In particular, the main aim of this study was to  
46 develop a cost-effective computational framework for designing gait rehabilitation patterns which (1)  
47 released the necessity of iterative MBD analysis and (2) directly calculated the specific kinematics needed  
48 to achieve a desired reduction in KCF.

## 49 **2. Materials and methods**

50 A published repository of the experimental gait cycles was obtained from the literature (section 2.1).  
51 The most influential gait kinematics for knee joint offloading and those body segment trajectories which  
52 control the overall lower limb alignments (constraints) were determined (section 2.2). Using the  
53 experimental repository, an artificial neural network was trained to predict the most influential gait  
54 kinematics (outputs) based on knee joint loading and constraint limb alignments (inputs) (section 2.3). The  
55 trained network was then employed to predict the appropriate waveforms of influential kinematics based on  
56 given patterns of knee joint loadings. Ground reaction forces and moments (GRF&M) were updated with  
57 respect to the proposed kinematic variations (section 2.4). In order to evaluate the efficiency and feasibility  
58 of the proposed kinematics, predicted kinematics and updated GRF&M were then imported into a MBD  
59 analysis to investigate whether the knee joint loading was decreased effectively (section 2.5). It should be

60 noted that artificial neural network was used for a twofold purpose: (1) to predict the synergetic kinematic  
61 variations needed to achieve a desired knee joint loading pattern (section 2.3) and (2) to update the  
62 GRF&M profile according to the kinematic variations (section 2.4). Figure 1 shows the schematic diagram  
63 of the proposed methodology.

## 64 **2.1. Subject**

65 A subject pool consisted of four different participants, implanted with unilateral sensor-based knee  
66 prostheses (three males, one female; height:  $168.3 \pm 2.6$  cm; mass:  $69.2 \pm 6.2$  kg), was adopted from a  
67 published repository (<https://simtk.org/home/kneeloads> ; accessed on 20 December 2013). This repository  
68 contained the experimental gait trials of seven different walking patterns: normal, bouncy, crouch, trunk  
69 sway and forefoot strike gait plus two knee rehabilitation strategies: medial thrust and walking pole patterns.  
70 Medial thrust pattern includes a slight decrease in pelvis obliquity and a slight increase in pelvis axial  
71 rotation and leg flexion compared to normal gait [13]. In walking pole gait, patient uses two lateral poles as  
72 supportive walking aids [17]. For each specific walking pattern, subjects repeated five gait trials under the  
73 same walking condition. One complete gait cycle was picked up for each gait trial. A gait cycle was defined  
74 as the time interval between foot strike of one leg to the following foot strike of the same leg [44]. Gait  
75 cycles were normalized to 100 samples and then averaged over each walking pattern, leading to a total  
76 number of 28 gait cycles for four participants. For a complete description of this repository one can refer to  
77 [45].

## 78 **2.2 Input/output selection**

### 79 **2.2.1. Input selection**

80 Presented in this study is a forward approach that is expected to directly predict the kinematic  
81 waveforms needed to implement a desired knee joint loading pattern. Medial and lateral components of  
82 desired KCF were considered as inputs. On the other hand, predicted kinematics should preserve the  
83 normal patterns of natural walking without any exaggerated limb orientation. Due to this constraint, those  
84 body segment trajectories which have been highly similar ( $\rho > 0.85$ ) across normal and natural-looking  
85 rehabilitation patterns (e.g., medial thrust and walking pole) were determined through Pearson correlation  
86 coefficients. These body segment trajectories were then considered as constraint inputs.

## 87 2.2.2. Output selection

88 In order to determine a specific gait modification, the most influential kinematics with significant  
89 contributions to the knee joint loading were chosen as outputs to be calculated. Reviewing previous studies,  
90 kernel mutual information (MI) has been used successfully as a nonlinear variable selection technique  
91 which releases the disadvantages of histogram-based MI [46]. This criterion was therefore recruited to  
92 measure the amount of information that each individual kinematic provided about knee joint loading [47]:

$$93 \quad I(X;Y) = \sum_{x_i \in X} \sum_{y_j \in Y} P(x_i, y_j) \log \frac{P(x_i, y_j)}{P(x_i)P(y_j)} \quad (1)$$

94 In the above equation, X refers to the input variable (medial KCF) whilst Y demonstrates the output  
95 variables (gait kinematics). Marginal probability of each variable (P(x), P(y)) and joint probability of input  
96 and output variables (P(x,y)) were calculated based on kernel density estimation as below [47]:

$$97 \quad P(y) = \frac{1}{n} \sum_{j=1}^N K(u) \quad (2)$$

98 Where

$$99 \quad u = \frac{(y - y_j)^T S^{-1} (y - y_j)}{h^2} \quad (3)$$

$$100 \quad K(u) = \frac{1}{2\pi^{\frac{d}{2}} h^2 \det(S)^{\frac{1}{2}}} \exp \frac{-u}{2} \quad (4)$$

$$101 \quad h = \left\{ \frac{4}{d+2} \right\}^{\frac{1}{d+4}} \times n^{\left\{ \frac{-1}{d+4} \right\}} \quad (5)$$

102 in which d is the vector dimension and S is the covariance matrix on  $y_j$ . It should be noted that unlike the  
103 previous applications of mutual information technique to select the inputs of a neural network[48], this  
104 technique was employed to determine the outputs of interest for the proposed neural network.

## 105 2.3. Artificial neural network

106 Feed forward artificial neural network (FFANN) has been widely accepted as a universal  
107 approximator [49]. This structure can learn any nonlinear relationship between inputs and outputs  
108 regardless of its complexity and dimension. In particular, FFANN was successfully used to predict knee  
109 joint loading patterns from gait kinematics in our previous study [43]. In the present study however,  
110 FFANN was used to solve the inverse of the former problem and predict the gait kinematics from knee joint  
111 loading patterns. The proposed FFANN consisted of a number of processor units (neurons) organized in

112 certain arrangements (layers). Layers were densely connected to each other via numeric weights [34].  
113 Once the neural network was trained for a specific nonlinear relationship, these numeric weights were  
114 adjusted to keep the “cause-and-effect” features of the input-output interaction [43]. All of the hidden  
115 neurons were activated by “hyperbolic tangent sigmoid” function whilst output nodes were activated with a  
116 “pure line” function which simply produced a weighted sum of hidden neurons in the output. Gradient  
117 descent back propagation algorithm with an adaptive learning rate (traingdx) and an error goal of  $10^{-5}$  were  
118 used to train the FFANN.

119 Experimental gait cycles of normal, bouncy, crouch, trunk sway and fore-foot strike patterns of all  
120 subjects were considered as the training data space (20 inter-patient data sets). This data space was  
121 randomly divided into three distinguished subsets: train (70%), validation (15%) and test (15%). Train and  
122 validation subsets were used to train the network and adjust the connection weights whilst the test subset  
123 was not included in the training procedure. The network prediction errors on the test and validation subsets  
124 were then considered to determine the optimum number of hidden neurons, hidden layers and training  
125 epochs. Whilst increasing the number of hidden neurons and layers would reduce the validation error, using  
126 too many hidden neurons and layers decrease the network generalization ability due to over-fitting and  
127 yield to an increase in prediction errors on the test subset [50]. This technique has been widely used in the  
128 literature to construct the optimal structure of a neural network [32, 33]. Training procedure continued until  
129 the maximum numbers of training epochs were reached or until the error goal was implemented. Once the  
130 trained network was validated and tested, it was then employed to calculate the appropriate kinematic  
131 waveforms (outputs) for a desired knee joint loading pattern (input). In this study, desired knee joint  
132 loading patterns were adopted from the medial thrust and walking pole trials. Subsequently, a five-layer  
133 FFANN with one input layer, three hidden layers (20, 25, 25 hidden neurons) and one output layer was  
134 constructed. This structure had 10 inputs (medial and lateral KCF plus eight constraint inputs) and four  
135 outputs (influential kinematics). Previous studies revealed the superiority of the FFANN compared to the  
136 regression surrogates for modeling complex nonlinear interactions [32, 37, 51]. In the present study, linear  
137 regression was also established for comparison purposes. All regression analyses were performed using  
138 MATLAB (v.2009, The MathWorks Inc.). A one-way analysis of variance (ANOVA) test with the  
139 significance level of  $p < 0.05$  was conducted (Matlab v.2009, Statistics toolbox) to compare the normalized  
140 root mean square errors between experimental kinematics (targets) and those predictions obtained from  
141 FFANN and regression surrogates for the test subset .

## 142 **2.4. Ground reaction force computations**

143 In general, three dimensional ground reaction forces and moments (GRF&M) are measured using  
144 force plates. However, GRF&M can also be calculated through a number of computational techniques [41,  
145 52, 53]. Here, an auxiliary four-layer FFANN with one input layer, two hidden layers (20 and 25 hidden  
146 neurons) and one output layer was constructed. This network had 15 inputs including 11 key values of  
147 predicted kinematic waveforms plus two peak and two impulse values of medial KCF in the midstance and  
148 terminal stance phases. These inputs are described in Table 1 and are shown in Figure 2. Midstance (17-  
149 50% of stance) and terminal stance (51-83% of stance) phases were defined based on the gait phase  
150 definitions by Perry and Burnfield [44] This FFANN had six output neurons to predict the peak values of  
151 ground reaction forces ( $F_x$ ,  $F_y$ , and  $F_z$ ) and ground reaction moments ( $M_x$ ,  $M_y$ , and  $M_z$ ). Hidden neurons'  
152 activation functions (hyperbolic tangent sigmoid), output neurons' activation functions (pure line) and  
153 training algorithm (gradient descent back propagation) were similar to the first FFANN in the previous  
154 section. The network was trained and validated based on the experimental gait cycles of normal , bouncy,  
155 crouch , trunk sway and fore foot strike gait trials (obtained from the published repository ; section 2.1).The  
156 trained structure was then employed to predict peak values of the GRF&M with respect to the proposed  
157 kinematic variations. Using linear interpolation technique (MATLAB software), the predicted peak values  
158 of GRF&M were used to re-scale and update an averaged ground reaction force profile of a normal gait  
159 cycle for each subject. This updated GRF&M profile accompanied the kinematic waveforms for further  
160 evaluation in MBD (section 2.5). Figure 3 outlines the sample input and output waveforms of the two  
161 neural networks used in this study.

## 162 **2.5 Multi-body dynamics evaluation**

163 For each subject, predicted gait kinematic waveforms (obtained from FFANN) were substituted in  
164 an averaged normal gait cycle of that subject (Appendix, Figure A.1) to generate a complete motion profile.  
165 This modified motion profile and updated GRF&M profile were then imported into the three-dimensional  
166 multi-body simulation software AnyBody Modeling System (version 5.2, AnyBody Technology, Aalborg,  
167 Denmark) to calculate the knee joint loading. The resultant knee joint loadings were expected to be lower  
168 than the resultant forces which were achieved from the original averaged normal gait cycle.

169 A lower extremity musculoskeletal model was used in AnyBody software based on the University  
170 of Twente Lower Extremity Model (TLEM) [54]. The TLEM model is available in the published repository



of AnyBody software. This model includes approximately 160 muscle units as well as thorax, trunk, pelvis, thigh, patella, shank and foot segments. Hip joint was modeled as a spherical joint with three degrees of freedom (DOF): flexion-extension, abduction-adduction and internal-external rotation. Knee joint was modeled as a hinge joint with only one DOF for flexion-extension and universal joint was considered for ankle-subtalar complex.

### 3. Results

In the present study, feed forward artificial neural network was employed to predict gait kinematics as outputs based on given knee joint loading patterns as inputs. Left heel, right lateral thigh, left inferior thigh, left lateral thigh, left patella, and left superior/inferior/lateral shank trajectories were highly correlated ( $p > 0.85$ ) between different natural-looking walking patterns (normal, medial thrust and walking pole patterns) (Figure 4). These body segment trajectories were therefore considered as constraint inputs to control the natural appearance and orientations of the predicted kinematics. Kernel mutual information also highlighted the significant contributions of four influential kinematics (kernel MI  $> 0.55$ ) to the knee joint loading including hip flexion, knee flexion, anterior-posterior and vertical components of pelvis position. These kinematic waveforms therefore were considered as outputs needed to be predicted by FFANN (Figure 5).

The predicted kinematics obtained from the regression surrogate model and FFANN were benchmarked versus experimental kinematic waveforms for the test subset (Appendix, Figure A.2). A significant difference of  $p = 3.8727e-005$  was found between the prediction accuracy of FFANN and regression surrogate in terms of the normalized root mean square errors. Accordingly, for the rest of this study, FFANN was considered. In addition, for comparison purposes and in order to show the importance of relevant constraint inputs to be chosen, FFANN predictions were repeated with all body segment trajectories as constraint inputs. This in turn resulted in a large increase in the prediction error on the test subset (up to 34%) (Appendix, Figure A.3).

Consequently, the trained FFANN with relevant constraint inputs (chosen through kernel MI) was employed to calculate the kinematic waveforms needed to achieve “desired knee joint loading” patterns. For each subject, kinematic waveforms were predicted corresponding to the knee joint loading patterns adopted from medial thrust (Figure 6) and walking pole (Figure 7) patterns as desired loading patterns. The auxiliary FFANN also predicted the peak values of GRF&M which were used to update the ground reaction force profiles for the medial thrust-based predicted kinematics (Figure 8) and walking pole-based predicted

201 kinematics (Figure 9). For brevity, adjusted GRF&M profiles are presented versus one representative  
202 normal gait cycle. For comparison purposes, FFANN-based updated GRF&M profile was compared versus  
203 the experimental GRF&M measurements of medial thrust pattern for subject 3 (Figure 8-b).

204 Feasibility and efficiency of the predicted gait kinematics were evaluated through MBD analysis  
205 (AnyBody software, section 2.5). For each subject, total knee joint loading was calculated based on the  
206 adjusted motion profiles (normal gait cycles in which predicted kinematic waveforms were substituted) and  
207 updated GRF&M profiles. Both medial thrust-based predicted kinematics and walking pole-based predicted  
208 kinematics could decrease the knee joint loading compared to the normal gait pattern (Figure 10). For  
209 comparison purposes, experimental kinematics of medial thrust and walking pole rehabilitation patterns,  
210 available in the published repository, were also imported into the MBD analysis. Computed total knee joint  
211 loadings are presented in Figure 10. Compared to normal walking pattern, medial thrust-based kinematics  
212 (predicted by FFANN) could decrease knee joint loading by 15%BW\*s and 23%BW\*s in the impulse  
213 values and by 19%BW and 22%BW in the peak values in the midstance and terminal stance phases.  
214 Walking pole-based kinematics (predicted by FFANN) also reduced knee joint loading by 19%BW\*s and  
215 25%BW\*s in the impulse values and by 21%BW and 28%BW in the peak values at the corresponding  
216 phases (averaged over four subjects) (Figure 11).

#### 217 **4. Discussion**

218 A feed forward artificial neural network was trained over a number of different gait trials and then  
219 was recruited to calculate the appropriate kinematics (outputs) for a given knee joint loading pattern  
220 (inputs). The FFANN structure was trained based on in vivo knee joint loadings obtained from instrumented  
221 knee prostheses. The proposed framework however, can also be trained using knee joint reaction forces  
222 computed through MBD analysis. Indeed all types of artificial neural networks require an initial  
223 computational expense to be trained over a primary training data space. The network learns the causal  
224 input-output interactions through this primary training data space. It should be pointed out that this initial  
225 cost would be much lower than the iterative “trial-and-error” analyses required in conventional  
226 rehabilitation designs using MBD analysis.

227 First, in each attempt of MBD analysis, the subject is hired to implement a gait pattern. The  
228 kinematic waveforms and GRF&M data are collected experimentally or calculated computationally to  
229 compute the resultant knee joint loading patterns. The design procedure is therefore established using an

230 inverse solution to obtain “force” from “kinematics”. Due to the unknown nonlinear interaction between  
231 gait kinematic variations and knee joint loading reduction, convergence of the solution may need numbers  
232 of attempts to achieve a reasonable reduction in the knee joint loading. Moreover, the solution and  
233 convergence probably differ from one subject to another. On the other hand, once a FFANN was trained  
234 based on a few numbers of gait trials (20 gait cycles for four subjects), it had the ability to directly calculate  
235 the appropriate kinematic waveforms from desired knee joint loading patterns (forward solution). Moreover,  
236 the trained FFANN could predict the corresponding kinematic variations for each of four different  
237 participants. Second, in order to produce a primary training data space for FFANN, several MBD analyses  
238 can be employed in parallel which may significantly reduce the required time of computations. In a  
239 conventional MBD-based rehabilitation design however, MBD analysis cannot be recruited in a parallel  
240 framework since the MBD computation results in each attempt specify how the kinematic waveforms and  
241 GRF&M profiles should be modified for the next attempt.

242 It should be pointed out that although a trained FFANN can learn and generalize a causal  
243 relationship to new situations, FFANN can only interpolate the training examples. In other words,  
244 predictions of FFANN are accurate and valid for those inputs which lay within the training data space. In  
245 the present study, the proposed FFANN was trained based on normal gait pattern as well as several  
246 exaggerated gait patterns (e.g., bouncy, crouch, fore foot strike and trunk sway). These gait patterns  
247 covered the span of executable gait patterns for each subject. Medial thrust and walking pole patterns (test  
248 data space) were natural-looking rehabilitation patterns with non-significant kinematic variations compared  
249 to normal gait. Thus, the kinematic waveforms of both patterns lay within the initial training data space.

250 The current approach is consistent with the previous studies for rehabilitation design in which a few  
251 influential gait kinematics are of particular interest to be varied while others are assumed to be normal [10,  
252 13, 14, 55, 56]. The rationale behind this technique can be justified according to two main reasons: (1) gait  
253 kinematics with low contributions to the knee joint loading, may have significant contributions to the  
254 adjacent joints (e.g. hip joint). Varying such kinematics may cause unwanted adverse changes in other  
255 joints loading patterns. As a conservative consideration therefore, targeted gait rehabilitations are mostly  
256 defined based on the minimum numbers of the kinematic variations. In other words, only those kinematics  
257 with significant influence on the knee joint loading should be altered; (2) after a rehabilitation strategy is  
258 designed theoretically, a patient should be trained clinically over the defined pattern. Fewer numbers of  
259 kinematic variations, required to be executed, will ease the training procedure. Extra facilities and attempts

260 will be required for patient training if the rehabilitation strategy involves more numbers of kinematic  
261 variations. In the present study, rehabilitation strategies were therefore suggested based upon four  
262 influential kinematic waveforms recognized through the kernel mutual information analysis.

263 Ground reaction forces mainly depend on the gravity, body mass and acceleration. Accordingly,  
264 variations in gait kinematics lead to unavoidable changes in GRF&M acting on the human body. Both  
265 kinematic variations and GRF&M changes in turn contribute to changes in the knee joint loading. In order  
266 to evaluate the predicted kinematic waveforms in a MBD analysis, GRF&M profiles should be updated. An  
267 auxiliary neural network was therefore constructed to update the peak values of GRF&M based on  
268 descriptive key values of the kinematic waveforms and desired knee joint loading patterns. These key  
269 values have been suggested in literature for a number of studies such as gait analysis [57-59], gait  
270 classification [60] and evaluation of joint loading [61], and joint inter-coordination [62]. Peak and  
271 impulse values of the knee joint loading in the midstance and terminal stance phases have also been used as  
272 important descriptive features of the knee joint loading in literature [13, 29, 36]. Predicted GRF&M profiles  
273 were in a good agreement with clinical reports [13]. For example, whilst statistical differences were  
274 reported to be noticeable between GRF&M profiles of walking pole and normal gait patterns (see Figure 9),  
275 GRF&M profiles of medial thrust were expected not to differ significantly from normal gait pattern (see  
276 Figure 8).

277 The FFANN-based framework suggested a forward solution for designing knee joint rehabilitation.  
278 Therefore, it can provide potential advantages and further insights into knee rehabilitation design. For  
279 example, kinematic waveforms predicted by FFANN, can serve as a starting point (initial guess) for  
280 conventional MBD-based designing approaches. Moreover, the FFANN framework can be fed with desired  
281 knee joint loading patterns which have not been achieved so far. For example, it is still not exactly clear  
282 whether any rehabilitation strategies can be designed to reduce knee joint loading at 25% of the stance  
283 phase. FFANN may be fed with a desired reduction at specific stages of a gait cycle. Estimated kinematics  
284 can then be evaluated clinically to investigate the possibility of a rehabilitation strategy capable of  
285 achieving this goal. As another example, knee joint loading patterns obtained from medial thrust and  
286 walking pole gaits can be combined and considered as the desired loading pattern (e.g., medial knee joint  
287 loading of medial thrust pattern plus lateral knee joint loading of walking pole rehabilitation) to investigate  
288 the feasibility of a compromised set of kinematics which inherits the potential advantages of both  
289 rehabilitation strategies.

290 One of the most important limitations of this study was lack of clinical investigation on estimated  
291 kinematics. However from a technical point of view, the predicted kinematic waveforms are expected to be  
292 feasible: (1) a total of eight body segment trajectories (constraint inputs) were considered to keep the  
293 natural orientation of the estimated kinematics; (2) the FFANN was trained based on executable walking  
294 patterns. Once the network learns this dynamics, it uses this dynamics as the acting function to respond to  
295 new sets of inputs. Due to the above reasons, it is unlikely that our model would generate highly aberrant  
296 kinematics. It should be noted that even if the predicted kinematics will be feasible to implement, further  
297 investigation is still necessary for compensatory or unexpected effects on the other joints or on the contra-  
298 lateral limb. The second limitation was that knee joint was modeled as a hinge joint with only one DOF  
299 (flexion-extension). Although six DOFs are possible for the knee joint , the dominant movement of the  
300 knee joint takes place in the sagittal plane, so a number of previous studies have modeled the knee as a  
301 hinge joint , especially for knee rehabilitation design purposes [13, 63, 64]. Nevertheless, the  
302 computational approach that was developed in the present study can be equally used with more complex  
303 musculoskeletal models. It should be noted that predicted kinematic waveforms were computationally  
304 replaced in an averaged normal gait cycle to generate a complete motion profile for MBD evaluation.  
305 Generally, after designing a gait rehabilitation strategy, based on a few kinematic variations, patients will  
306 be asked to execute the prescribed kinematics in their gait patterns. Other gait kinematics, which are not  
307 prescribed in the rehabilitation strategy, will be therefore synchronized while patient is walking. In the  
308 present study however we mainly aimed to introduce the computational approach (FFANN) for gait  
309 modification designs. Due to lack of experimental set-up and clinical validation, predicted kinematic  
310 waveforms were only computationally replaced in a normal gait cycle to be evaluated in a MBD approach.  
311 Nevertheless, the results are not expected to vary noticeably since the predicted kinematics does not differ  
312 significantly from normal gait patterns (see Figures 5 and 6). Finally it should be pointed out that no special  
313 assumption was made to include or exclude a participant. In other words, the proposed computational  
314 framework was constructed based on a few numbers of ordinary subjects with unilateral knee implants. The  
315 proposed methodology is therefore expected to be equally applicable for any given subject. However, for  
316 patients with abnormal varus or valgus knee joint alignment , pathologic gait patterns or those subjects with  
317 other joint diseases , other gait trials may be needed to train the neural network. Caution is required to train  
318 subjects on the predicted kinematics and further clinical validation should be carried out to investigate other  
319 effects of the proposed kinematics on the other joints.

## 320 **5. Conclusions**

321 A FFANN-based computational framework was developed to calculate the appropriate kinematic  
322 waveforms needed to achieve desired knee joint loadings corresponding to medial thrust and walking pole  
323 patterns. Evaluating the predicted kinematic waveforms in a multi-body dynamics analysis, impulse values  
324 of the knee joint loadings, with respect to bodyweight (BW), were decreased by 17%BW\*s and 24%BW\*s  
325 in the midstance and the terminal stance phases. Peak values of the knee joint loadings were also reduced  
326 by 20%BW and 25%BW at the corresponding phases. This computational framework provided a cost-  
327 effective approach capable of designing gait rehabilitation strategies for individual subjects which released  
328 the necessity of iterative multi-body dynamic analysis.

### 329 **Conflict of interest statement**

330 The authors have no conflict of interests to be declared.

### 331 **Acknowledgement**

332 This work was supported by “the Fundamental Research Funds for the Central Universities”,  
333 National Natural Science Foundation of China [E050702,51323007] , the program of Xi’an Jiao Tong  
334 University [grant number xjj2012108], and the program of Kaifang funding of the State Key Lab for  
335 Manufacturing Systems Engineering [grant number sklms2011001].

## **References**

- 336 [1] M. Hurley, D. Scott, Improvements in quadriceps sensorimotor function and disability of patients with  
337 knee osteoarthritis following a clinically practicable exercise regime, *Rheumatology*, 37 (1998) 1181-1187.
- 338 [2] H. Røggind, B. Bibow-Nielsen, B. Jensen, H.C. Møller, H. Frimodt-Møller, H. Bliddal, The effects of a physical  
339 training program on patients with osteoarthritis of the knees, *Archives of physical medicine and rehabilitation*,  
340 79 (1998) 1421-1427.
- 341 [3] D. Isaac, T. Falode, P. Liu, H. I'Anson, K. Dillow, P. Gill, Accelerated rehabilitation after total knee  
342 replacement, *The knee*, 12 (2005) 346-350.
- 343 [4] G.R. Klein, H.B. Levine, M.A. Hartzband, Pain Management and Accelerated Rehabilitation After Total Knee  
344 Arthroplasty, *Seminars in Arthroplasty*, (Elsevier2008), pp. 248-251.
- 345 [5] H. Moffet, J.-P. Collet, S.H. Shapiro, G. Paradis, F. Marquis, L. Roy, Effectiveness of intensive rehabilitation on  
346 functional ability and quality of life after first total knee arthroplasty: a single-blind randomized controlled  
347 trial, *Archives of physical medicine and rehabilitation*, 85 (2004) 546-556.
- 348 [6] A.E. Rahmann, S.G. Brauer, J.C. Nitz, A specific inpatient aquatic physiotherapy program improves strength  
349 after total hip or knee replacement surgery: a randomized controlled trial, *Archives of physical medicine and  
350 rehabilitation*, 90 (2009) 745-755.
- 351 [7] J. Zeni Jr, J. McClelland, L. Snyder-Mackler, 193 A NOVEL REHABILITATION PARADIGM TO IMPROVE  
352 MOVEMENT SYMMETRY AND MAXIMIZE LONG-TERM OUTCOMES AFTER TOTAL KNEE ARTHROPLASTY,  
353 *Osteoarthritis and Cartilage*, 19 (2011) S96-S97.
- 354 [8] M. Fransen, Rehabilitation after knee replacement surgery for osteoarthritis, *Seminars in Arthritis and  
355 Rheumatism*, (Elsevier2011), pp. 93.
- 356 [9] M.A. Mont, P.M. Bonutti, T.M. Seyler, J.F. Plate, R.E. Delanois, M. Kester, The future of high performance total  
357 hip arthroplasty, *Seminars in Arthroplasty*, (Elsevier2006), pp. 88-92.
- 358 [10] J.A. Barrios, K.M. Crossley, I.S. Davis, Gait retraining to reduce the knee adduction moment through real-  
359 time visual feedback of dynamic knee alignment, *Journal of biomechanics*, 43 (2010) 2208-2213.
- 360 [11] B.J. Fregly, Computational assessment of combinations of gait modifications for knee osteoarthritis  
361 rehabilitation, *Biomedical Engineering, IEEE Transactions on*, 55 (2008) 2104-2106.
- 362 [12] B.J. Fregly, D.D. D'Lima, C.W. Colwell, Effective gait patterns for offloading the medial compartment of the  
363 knee, *Journal of Orthopaedic Research*, 27 (2009) 1016-1021.
- 364 [13] B.J. Fregly, J.A. Reinbolt, K.L. Rooney, K.H. Mitchell, T.L. Chmielewski, Design of patient-specific gait  
365 modifications for knee osteoarthritis rehabilitation, *Biomedical Engineering, IEEE Transactions on*, 54 (2007)  
366 1687-1695.
- 367 [14] M.A. Hunt, M. Simic, R.S. Hinman, K.L. Bennell, T.V. Wrigley, Feasibility of a gait retraining strategy for  
368 reducing knee joint loading: increased trunk lean guided by real-time biofeedback, *Journal of biomechanics*, 44  
369 (2011) 943-947.
- 370 [15] A. Mündermann, C.O. Dyrby, D.E. Hurwitz, L. Sharma, T.P. Andriacchi, Potential strategies to reduce medial  
371 compartment loading in patients with knee osteoarthritis of varying severity: reduced walking speed, *Arthritis  
372 & Rheumatism*, 50 (2004) 1172-1178.
- 373 [16] P.B. Shull, R. Shultz, A. Silder, J.L. Dragoo, T.F. Besier, M.R. Cutkosky, S.L. Delp, Toe-in gait reduces the first  
374 peak knee adduction moment in patients with medial compartment knee osteoarthritis, *Journal of  
375 biomechanics*, (2012).
- 376 [17] J. Willson, M.R. Torry, M.J. Decker, T. Kernozek, J. Steadman, Effects of walking poles on lower extremity  
377 gait mechanics, *Medicine and science in sports and exercise*, 33 (2001) 142-147.
- 378 [18] J.A. Barrios, I.S. Davis, A gait modification to reduce the external adduction moment at the knee: a case  
379 study, 31st Annual Meeting of the American Society of Biomechanics, Stanford, CA, paper2007).
- 380 [19] M. Hunt, T. Birmingham, D. Bryant, I. Jones, J. Giffin, T. Jenkyn, A. Vandervoort, Lateral trunk lean explains  
381 variation in dynamic knee joint load in patients with medial compartment knee osteoarthritis, *Osteoarthritis  
382 and Cartilage*, 16 (2008) 591-599.

383 [20] M. Simic, R.S. Hinman, T.V. Wrigley, K.L. Bennell, M.A. Hunt, Gait modification strategies for altering  
384 medial knee joint load: A systematic review, *Arthritis Care & Research*, 63 (2011) 405-426.

385 [21] B.D. Street, W. Gage, The effects of an adopted narrow gait on the external adduction moment at the knee  
386 joint during level walking: Evidence of asymmetry, *Human movement science*, (2013).

387 [22] J.C. van den Noort, I. Schaffers, J. Snijders, J. Harlaar, The effectiveness of voluntary modifications of gait  
388 pattern to reduce the knee adduction moment, *Human movement science*, (2013).

389 [23] I. Kutzner, B. Heinlein, F. Graichen, A. Bender, A. Rohlmann, A. Halder, A. Beier, G. Bergmann, Loading of  
390 the knee joint during activities of daily living measured in vivo in five subjects, *Journal of*  
391 *biomechanics*, 43 (2010) 2164-2173.

392 [24] W.R. Taylor, M.O. Heller, G. Bergmann, G.N. Duda, Tibio-femoral loading during human gait and stair  
393 climbing, *Journal of Orthopaedic Research*, 22 (2004) 625-632.

394 [25] S.K. Lynn, P.A. Costigan, Effect of foot rotation on knee kinetics and hamstring activation in older adults  
395 with and without signs of knee osteoarthritis, *Clinical Biomechanics*, 23 (2008) 779-786.

396 [26] C.-J. Lin, K.-A. Lai, Y.-L. Chou, C.-S. Ho, The effect of changing the foot progression angle on the knee  
397 adduction moment in normal teenagers, *Gait & Posture*, 14 (2001) 85-91.

398 [27] M.W. Creaby, M.A. Hunt, R.S. Hinman, K.L. Bennell, Sagittal plane joint loading is related to knee flexion in  
399 osteoarthritic gait, *Clinical Biomechanics*, 28 (2013) 916-920.

400 [28] D. Zhao, S.A. Banks, K.H. Mitchell, D.D. D'Lima, C.W. Colwell, B.J. Fregly, Correlation between the knee  
401 adduction torque and medial contact force for a variety of gait patterns, *Journal of Orthopaedic Research*, 25  
402 (2007) 789-797.

403 [29] J.P. Walter, D.D. D'Lima, C.W. Colwell, B.J. Fregly, Decreased knee adduction moment does not guarantee  
404 decreased medial contact force during gait, *Journal of Orthopaedic Research*, 28 (2010) 1348-1354.

405 [30] N. Arjmand, O. Ekrami, A. Shirazi-Adl, A. Plamondon, M. Parnianpour, Relative performances of artificial  
406 neural network and regression mapping tools in evaluation of spinal loads and muscle forces during static  
407 lifting, *Journal of Biomechanics*, 46 (2013) 1454-1462.

408 [31] G. Campoli, H. Weinans, A.A. Zadpoor, Computational load estimation of the femur, *Journal of the*  
409 *Mechanical Behavior of Biomedical Materials*, 10 (2012) 108-119.

410 [32] Y. Lu, P.R. Pulasani, R. Derakhshani, T.M. Guess, Application of neural networks for the prediction of  
411 cartilage stress in a musculoskeletal system, *Biomedical Signal Processing and Control*, 8 (2013) 475-482.

412 [33] A.A. Zadpoor, G. Campoli, H. Weinans, Neural network prediction of load from the morphology of  
413 trabecular bone, *Applied Mathematical Modelling*, (2012).

414 [34] S.S. Haykin, S.S. Haykin, S.S. Haykin, S.S. Haykin, *Neural networks and learning machines* (Prentice Hall  
415 New York, 2009).

416 [35] M.M. Ardestani, X. Zhang, L. Wang, Q. Lian, Y. Liu, J. He, D. Li, Z. Jin, Human lower extremity joint moment  
417 prediction: A wavelet neural network approach, *Expert Systems with Applications*, (2013).

418 [36] J. Favre, M. Hayoz, J.C. Erhart-Hledik, T.P. Andriacchi, A neural network model to predict knee adduction  
419 moment during walking based on ground reaction force and anthropometric measurements, *Journal of*  
420 *biomechanics*, 45 (2012) 692-698.

421 [37] M.E. Hahn, Feasibility of estimating isokinetic knee torque using a neural network model, *Journal of*  
422 *biomechanics*, 40 (2007) 1107-1114.

423 [38] Y. Liu, S.-M. Shih, S.-L. Tian, Y.-J. Zhong, L. Li, Lower extremity joint torque predicted by using artificial  
424 neural network during vertical jump, *Journal of biomechanics*, 42 (2009) 906-911.

425 [39] F. Zhang, P. Li, Z.-G. Hou, Z. Lu, Y. Chen, Q. Li, M. Tan, sEMG-based continuous estimation of joint angles of  
426 human legs by using BP neural network, *Neurocomputing*, 78 (2012) 139-148.

427 [40] D. Billing, C. Nagarajah, J. Hayes, J. Baker, Predicting ground reaction forces in running using micro-  
428 sensors and neural networks, *Sports Engineering*, 9 (2006) 15-27.



- 429 [41] S.E. Oh, A. Choi, J.H. Mun, Prediction of ground reaction forces during gait based on kinematics and a  
430 neural network model, *Journal of biomechanics*, 46 (2013) 2372-2380.
- 431 [42] H. Savelberg, A. De Lange, Assessment of the horizontal, fore-aft component of the ground reaction force  
432 from insole pressure patterns by using artificial neural networks, *Clinical Biomechanics*, 14 (1999) 585-592.
- 433 [43] M.M. Ardestani, Z. Chen, L. Wang, Q. Lian, Y. Liu, J. He, D. Li, Z. Jin, Feed forward artificial neural network to  
434 predict contact force at medial knee joint: Application to gait modification, *Neurocomputing*, (2014).
- 435 [44] J. Perry, J.M. Burnfield, *Gait analysis: normal and pathological function* (Slack, 1993).
- 436 [45] B.J. Fregly, T.F. Besier, D.G. Lloyd, S.L. Delp, S.A. Banks, M.G. Pandy, D.D. D'Lima, Grand challenge  
437 competition to predict in vivo knee loads, *Journal of Orthopaedic Research*, 30 (2012) 503-513.
- 438 [46] B.V. Bonnlander, A.S. Weigend, Selecting input variables using mutual information and nonparametric  
439 density estimation, *Proceedings of the 1994 International Symposium on Artificial Neural Networks*  
440 (ISANN'94), (Citeseer1994), pp. 42-50.
- 441 [47] Y.-I. Moon, B. Rajagopalan, U. Lall, Estimation of mutual information using kernel density estimators,  
442 *Physical Review E*, 52 (1995) 2318.
- 443 [48] R. May, G. Dandy, H. Maier, Review of input variable selection methods for artificial neural networks,  
444 *Artificial neural networks—methodological advances and biomedical applications*. InTech, Croatia. doi, 10  
445 (2011) 16004.
- 446 [49] A.R. Barron, Universal approximation bounds for superpositions of a sigmoidal function, *Information*  
447 *Theory, IEEE Transactions on*, 39 (1993) 930-945.
- 448 [50] E. Alpaydin, *Introduction to Machine Learning (Adaptive Computation and Machine Learning Series)*,  
449 (The MIT Press Cambridge2004).
- 450 [51] W. Youn, J. Kim, Feasibility of using an artificial neural network model to estimate the elbow flexion force  
451 from mechanomyography, *Journal of neuroscience methods*, 194 (2011) 386-393.
- 452 [52] L. Ren, R.K. Jones, D. Howard, Whole body inverse dynamics over a complete gait cycle based only on  
453 measured kinematics, *Journal of Biomechanics*, 41 (2008) 2750-2759.
- 454 [53] Y. Xiang, J.S. Arora, K. Abdel-Malek, Optimization-based prediction of asymmetric human gait, *Journal of*  
455 *biomechanics*, 44 (2011) 683-693.
- 456 [54] M.D. Klein Horsman, *The Twente lower extremity model: consistent dynamic simulation of the human*  
457 *locomotor apparatus* (University of Twente, 2007).
- 458 [55] T. Kraus, M. Švehlík, G. Steinwender, W. Linhart, E. Zwick, Gait modifications to unload the hip in children  
459 with Legg–Calve–Perthes disease, *Gait & Posture*, 36 (2012) S92-S93.
- 460 [56] C.L. Lewis, S.A. Sahrman, D.W. Moran, Effect of hip angle on anterior hip joint force during gait, *Gait &*  
461 *posture*, 32 (2010) 603-607.
- 462 [57] T.D. Collins, S.N. Ghoussayni, D.J. Ewins, J.A. Kent, A six degrees-of-freedom marker set for gait analysis:  
463 repeatability and comparison with a modified Helen Hayes set, *Gait & posture*, 30 (2009) 173-180.
- 464 [58] D.H. Gates, J.B. Dingwell, S.J. Scott, E.H. Sinitiski, J.M. Wilken, Gait characteristics of individuals with  
465 transtibial amputations walking on a destabilizing rock surface, *Gait & posture*, 36 (2012) 33-39.
- 466 [59] D.H. Gates, J.M. Wilken, S.J. Scott, E.H. Sinitiski, J.B. Dingwell, Kinematic strategies for walking across a  
467 destabilizing rock surface, *Gait & Posture*, 35 (2012) 36-42.
- 468 [60] S. Armand, E. Watelain, M. Mercier, G. Lensele, F.-X. Lepoutre, Identification and classification of toe-  
469 walkers based on ankle kinematics, using a data-mining method, *Gait & posture*, 23 (2006) 240-248.
- 470 [61] E.B. Simonsen, L.M. Moesby, L.D. Hansen, J. Comins, T. Alkjaer, Redistribution of joint moments during  
471 walking in patients with drop-foot, *Clinical Biomechanics*, 25 (2010) 949-952.
- 472 [62] T.-M. Wang, H.-C. Yen, T.-W. Lu, H.-L. Chen, C.-F. Chang, Y.-H. Liu, W.-C. Tsai, Bilateral knee osteoarthritis  
473 does not affect inter-joint coordination in older adults with gait deviations during obstacle-crossing, *Journal of*  
474 *biomechanics*, 42 (2009) 2349-2356.

- 475 [63] M. Ackermann, A.J. van den Bogert, Optimality principles for model-based prediction of human gait,  
476 Journal of biomechanics, 43 (2010) 1055-1060.
- 477 [64] F.C. Anderson, M.G. Pandy, Dynamic optimization of human walking, TRANSACTIONS-AMERICAN  
478 SOCIETY OF MECHANICAL ENGINEERS JOURNAL OF BIOMECHANICAL ENGINEERING, 123 (2001) 381-390.  
479

Figure 1

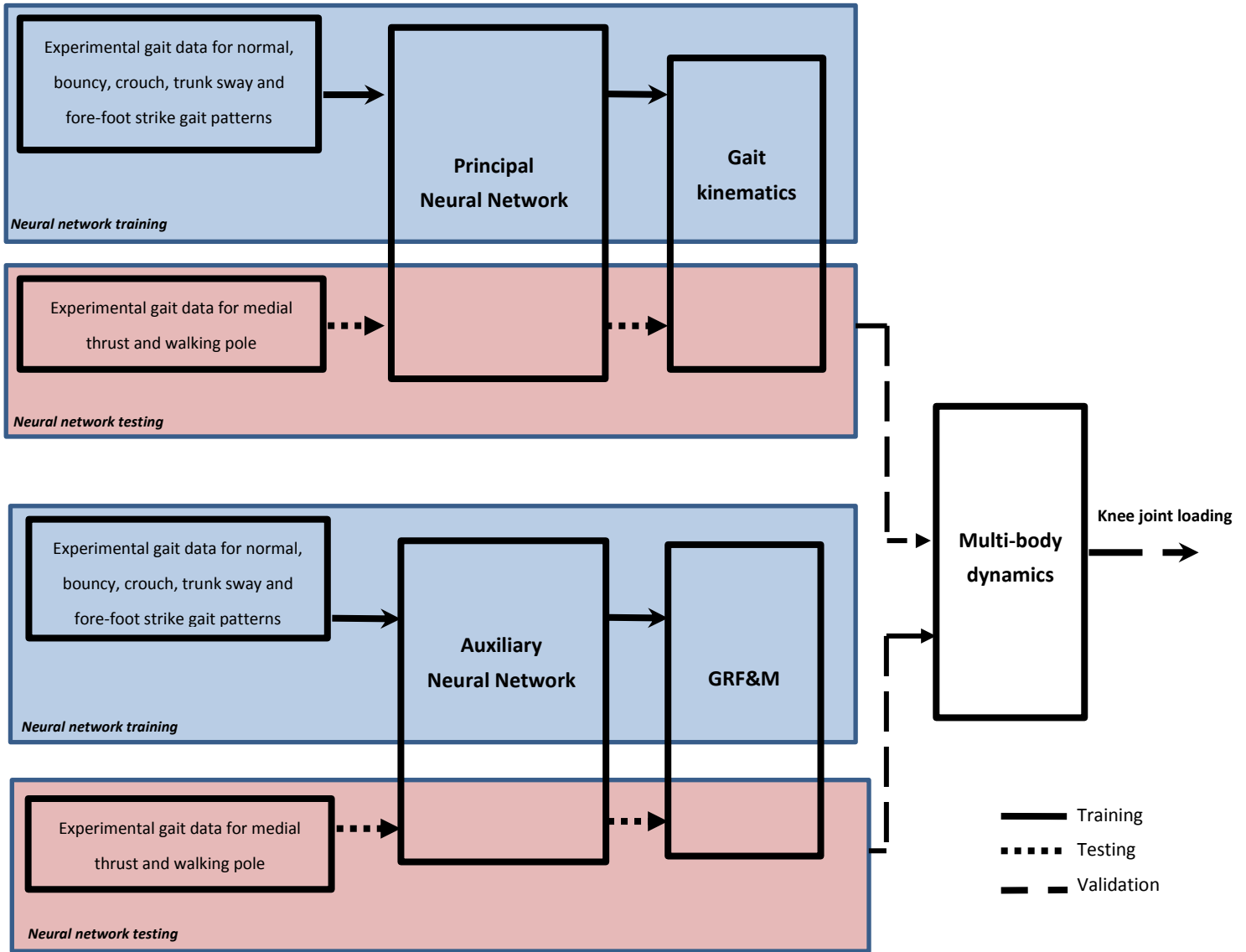


Figure 1 A schematic block diagram of the proposed framework

**Figure 2**

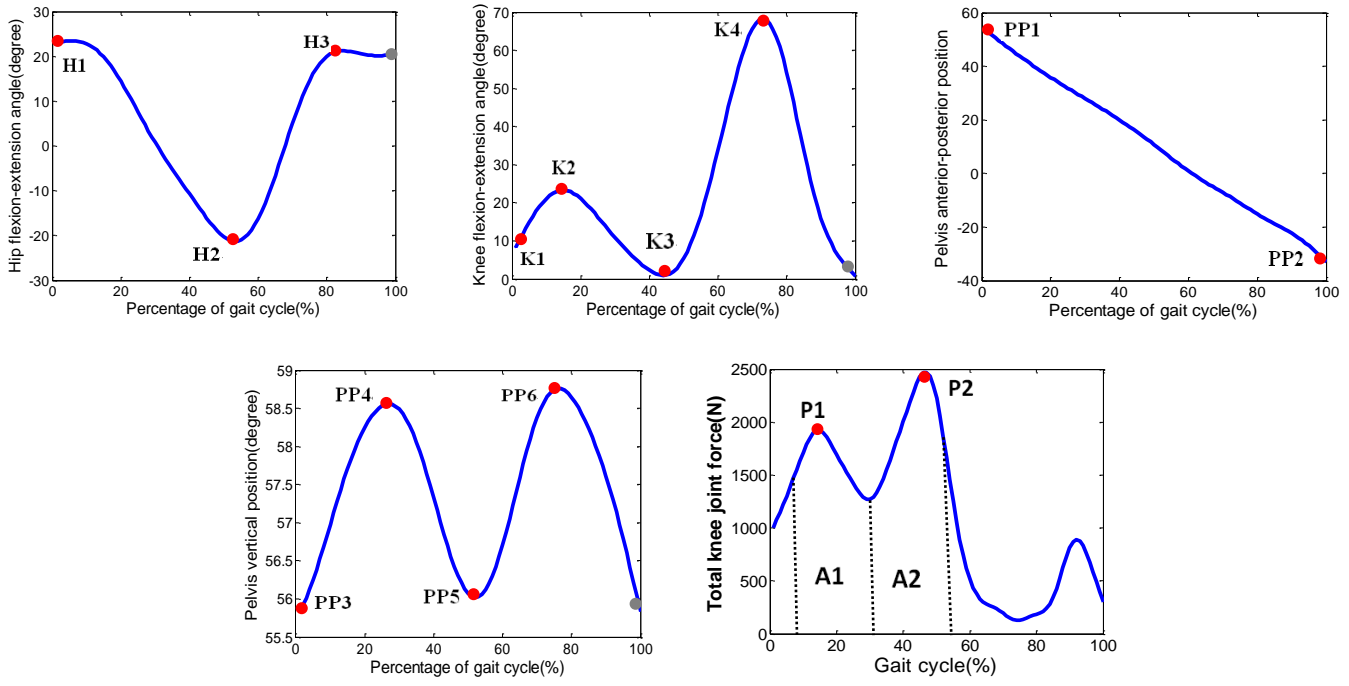


Figure 2 Input variables of the auxiliary FFANN (red circles) including key values of the predicted gait kinematics plus peak & impulse values of the desired medial KCF. Due to the periodicity of the gait, kinematic values at the end of the gait cycle (gray points) were equal to the initial values at 0% of the gait cycle; except for pelvis anterior-posterior translation.

Figure 3

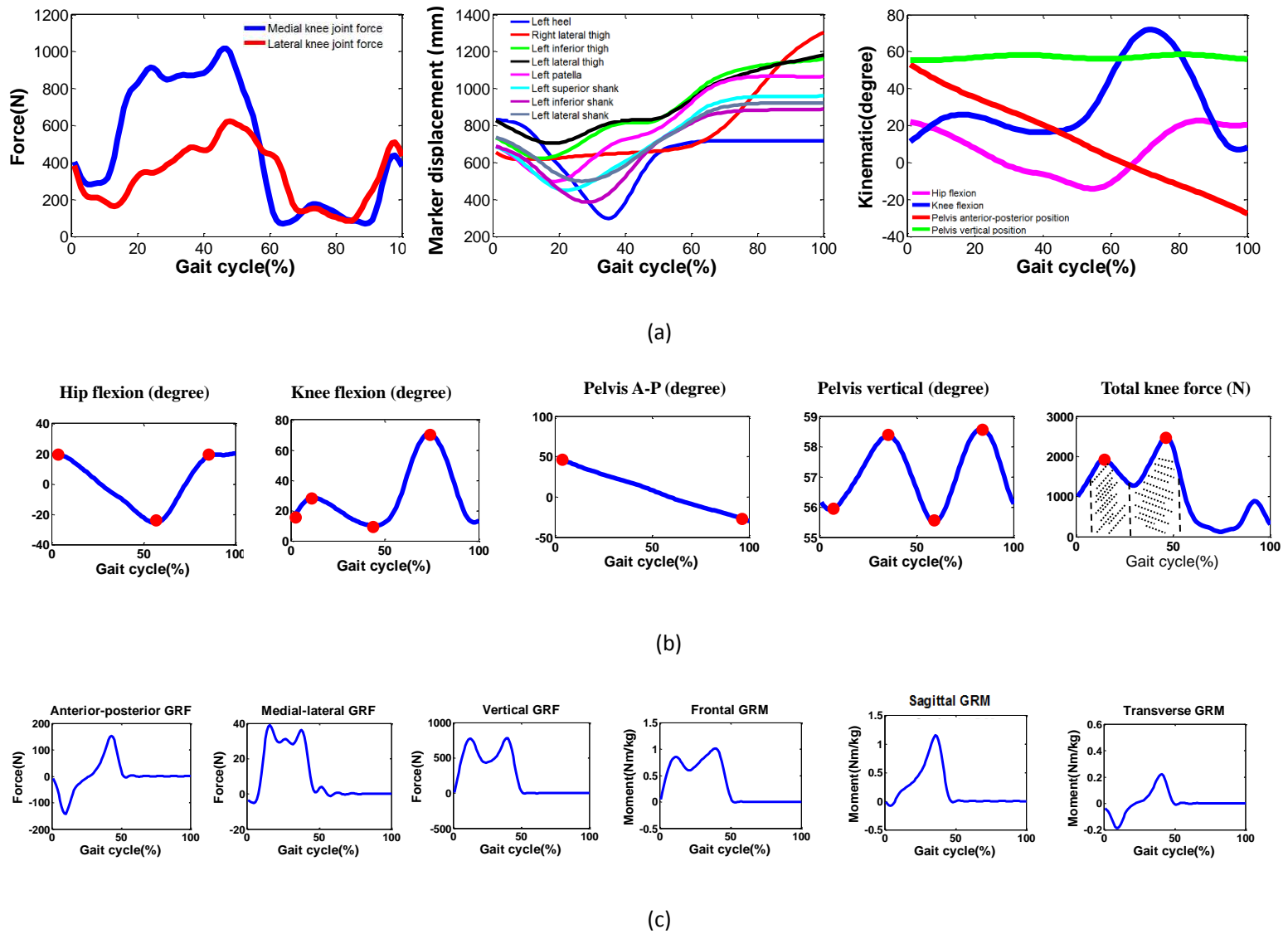


Figure 3 (a) Sample input and output waveforms for the principal FFANN. Medial and lateral knee joint forces plus marker displacement trajectories served as inputs to predict kinematics as outputs, (b) descriptive features of kinematics and kinetics which served as input variables for the auxiliary FFANN, (c) GRF&M profile as outputs of the auxiliary FFANN.

Figure 4

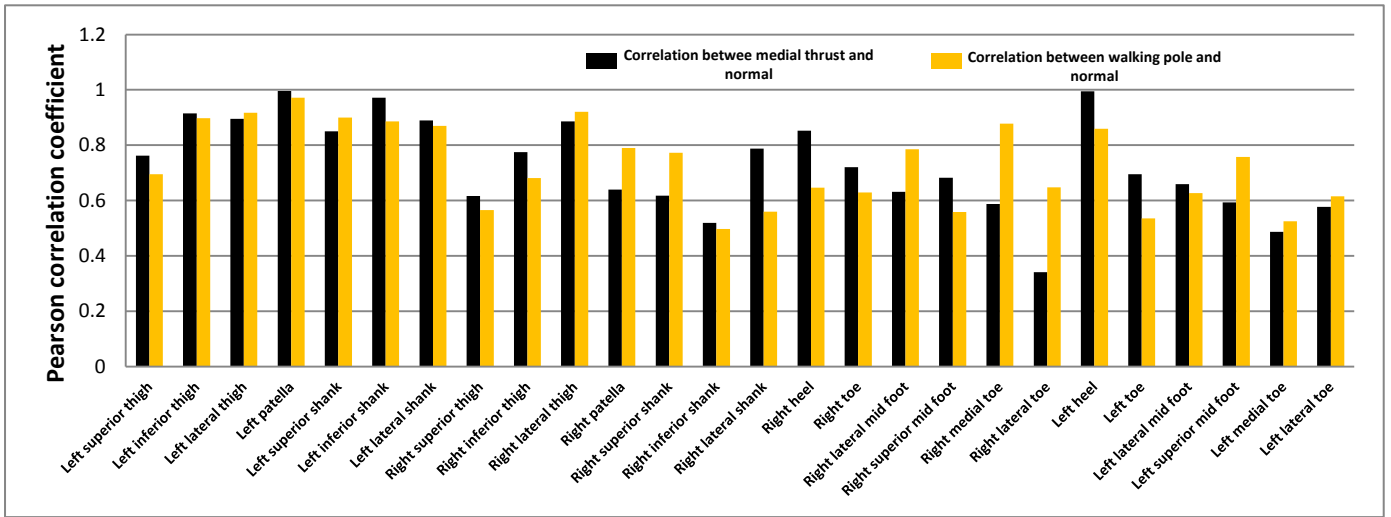


Figure 4 Pearson correlation coefficients were calculated across different body segment trajectories over different natural-looking walking patterns (normal, medial thrust and walking pole patterns)

Figure 5

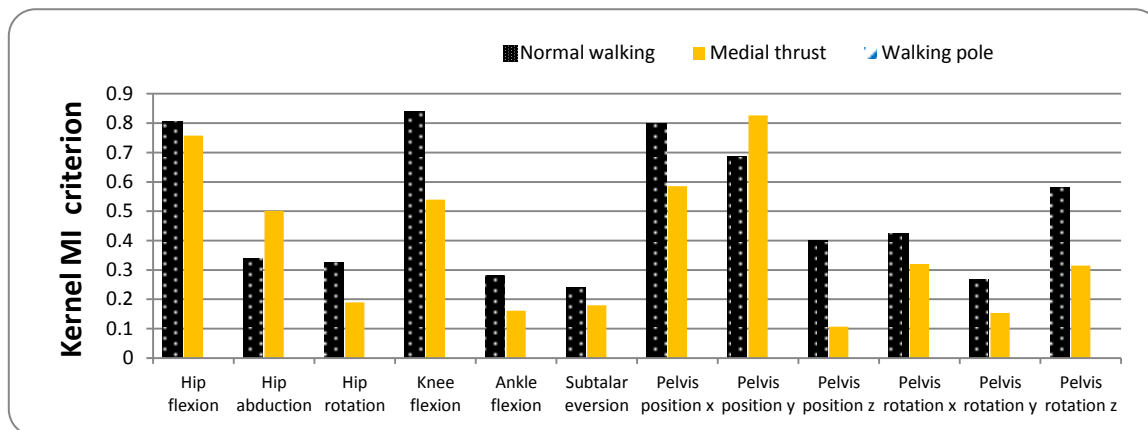


Figure 5 Kernel mutual information values between gait kinematics and medial KCF; x, y and z refer to anterior-posterior, vertical and medial-lateral directions.

Figure 6

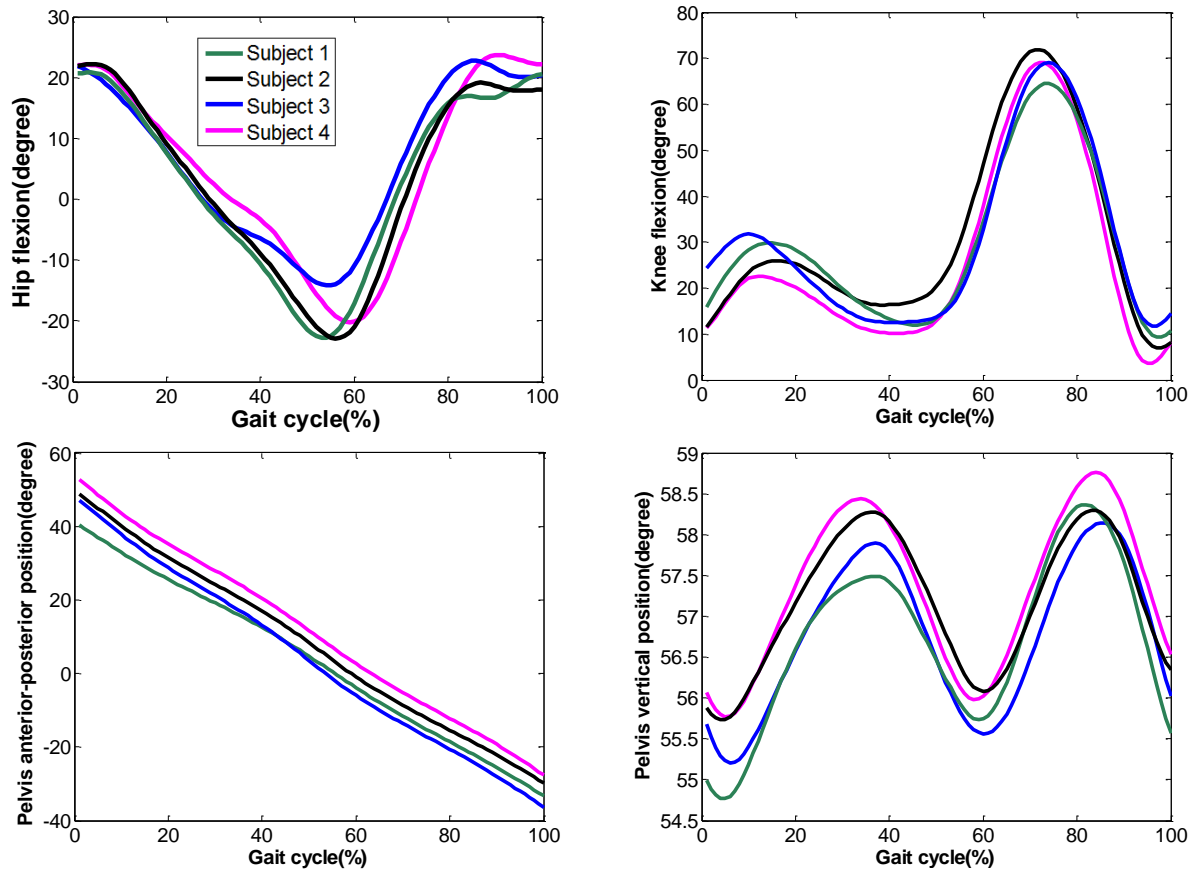


Figure 6 Predicted kinematic waveforms (outputs) corresponding to the knee joint loading patterns adopted from the medial thrust rehabilitation strategy (inputs).



Figure 7

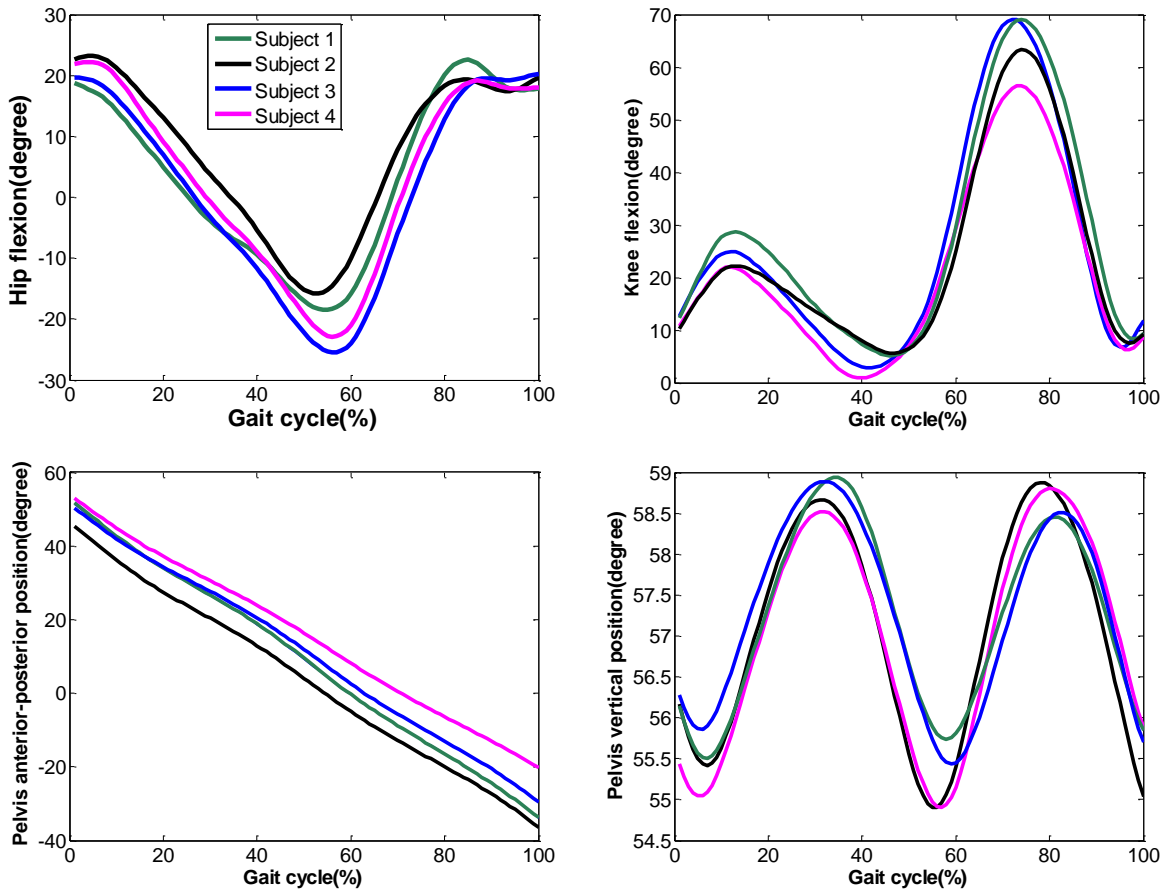


Figure 7 Predicted kinematic waveforms (outputs) corresponding to the knee joint loading patterns adopted from the walking pole rehabilitation strategy (inputs).

Figure 8

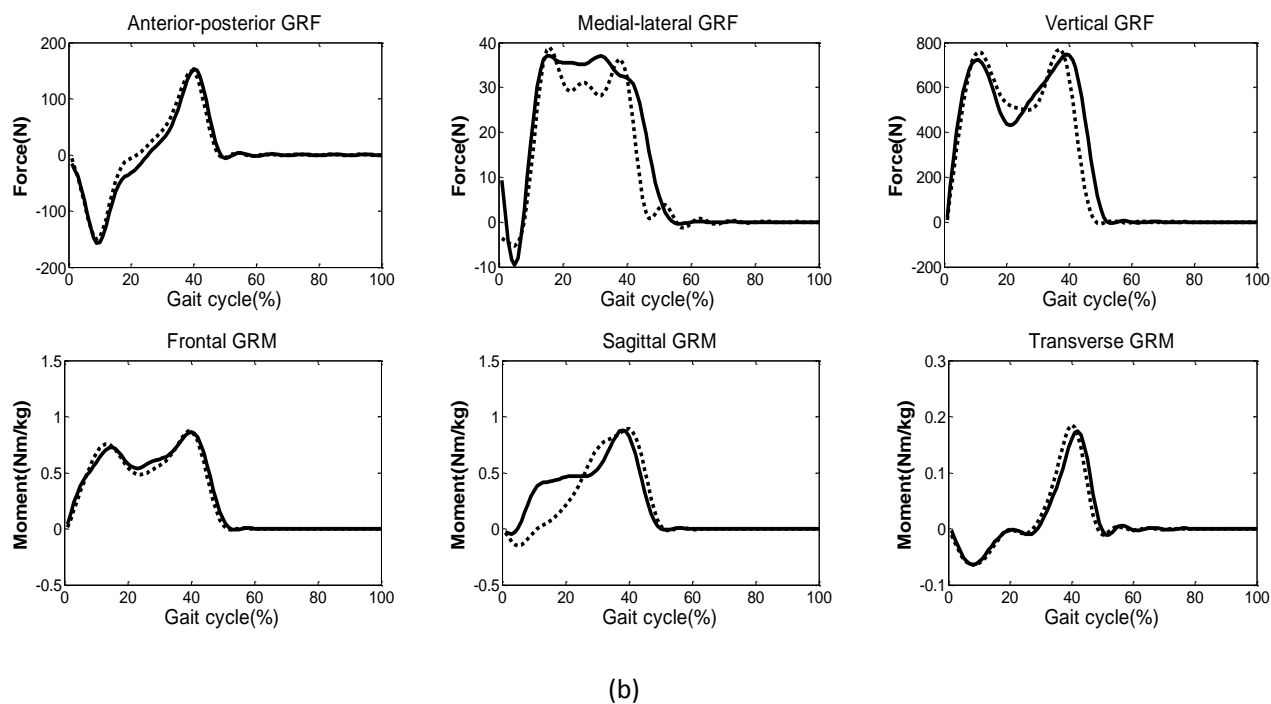
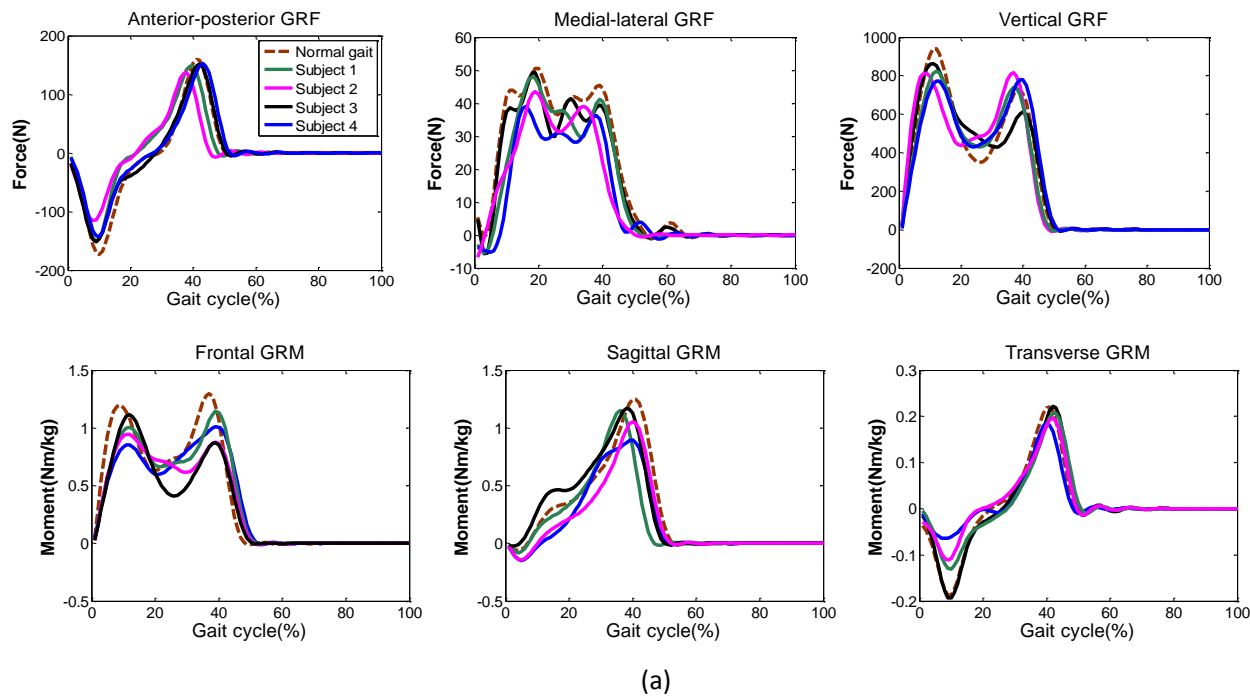


Figure 8 (a) Updated ground reaction force and moment profiles corresponding to the medial thrust-based predicted kinematics, (b) FFANN-based updated GRF&M was compared versus the corresponding experimental measurements of medial thrust pattern for subject 3 as an example.

Figure 9

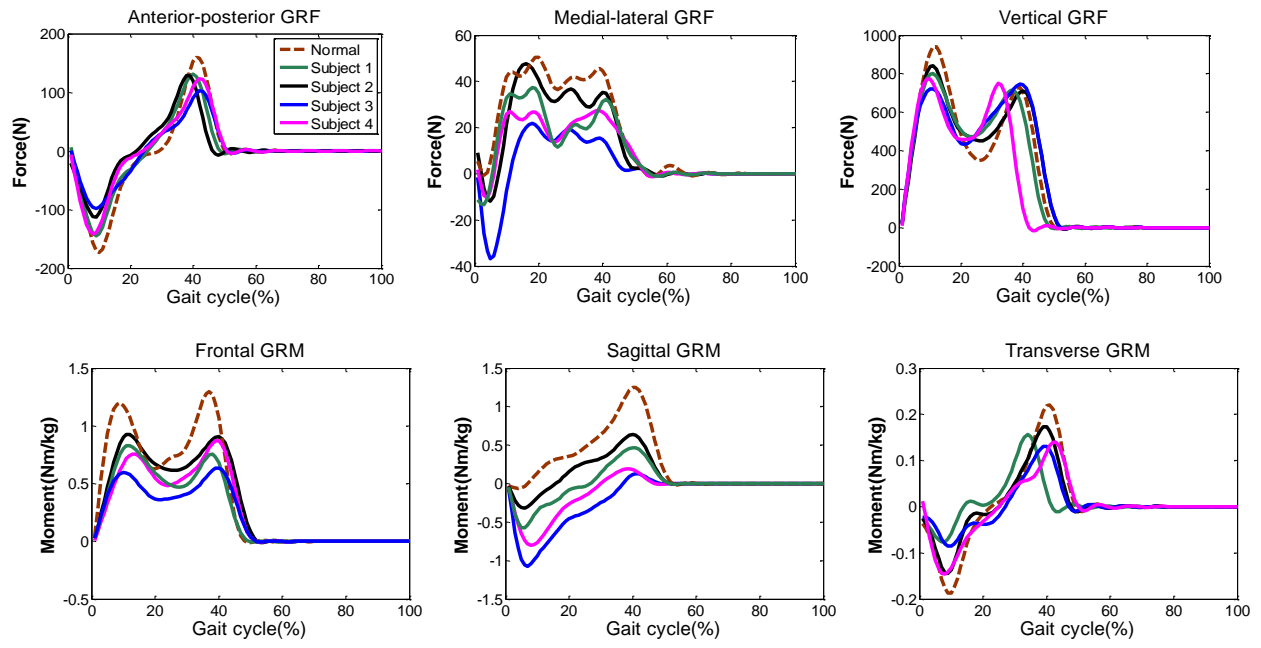


Figure 9 Updated ground reaction force and moment profiles corresponding to the walking pole-based predicted kinematics.

Figure 10

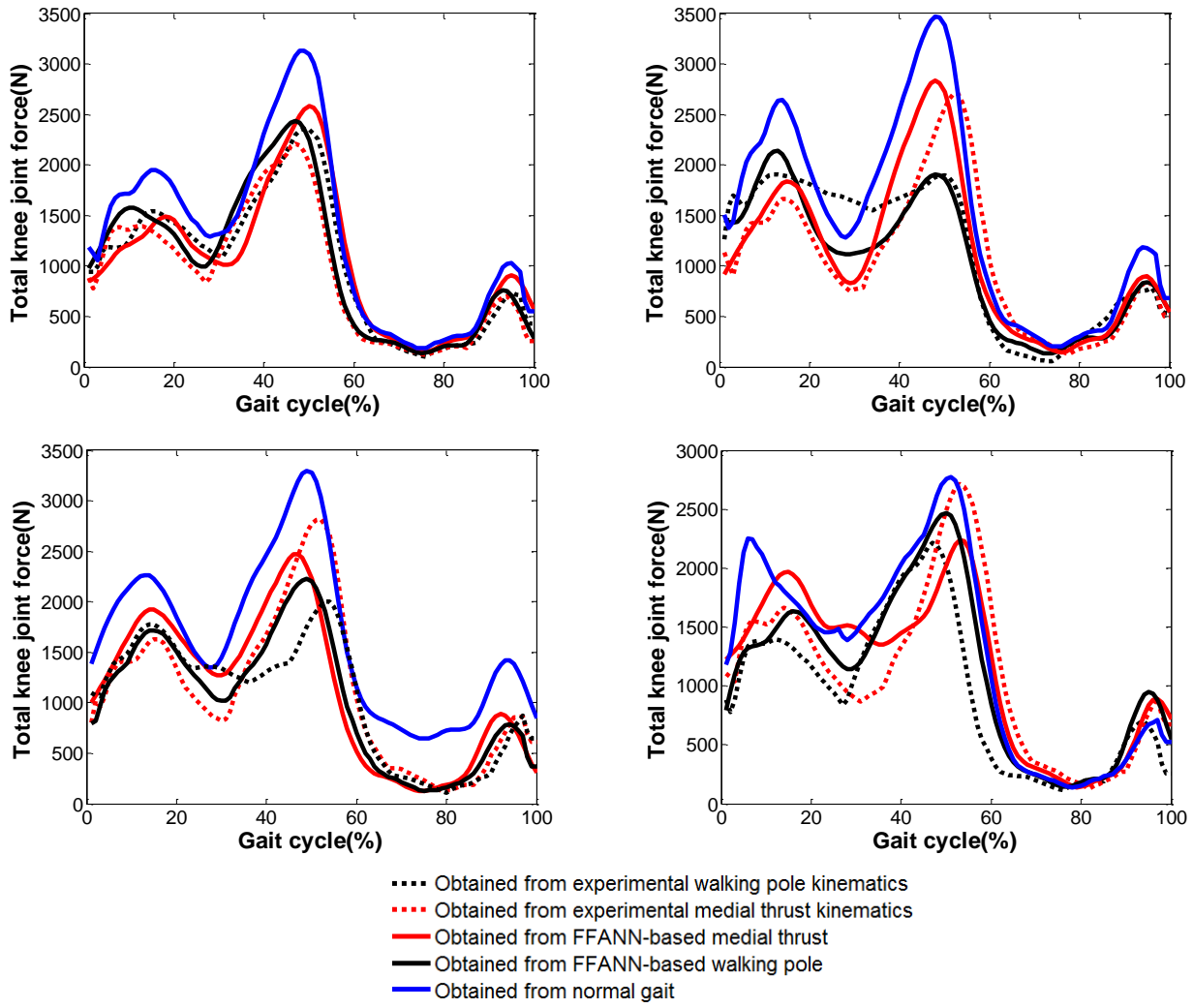


Figure 10 Both medial thrust-based predicted kinematics and walking pole-based predicted kinematics could decrease the knee joint loading compared to the normal gait pattern

Figure 11

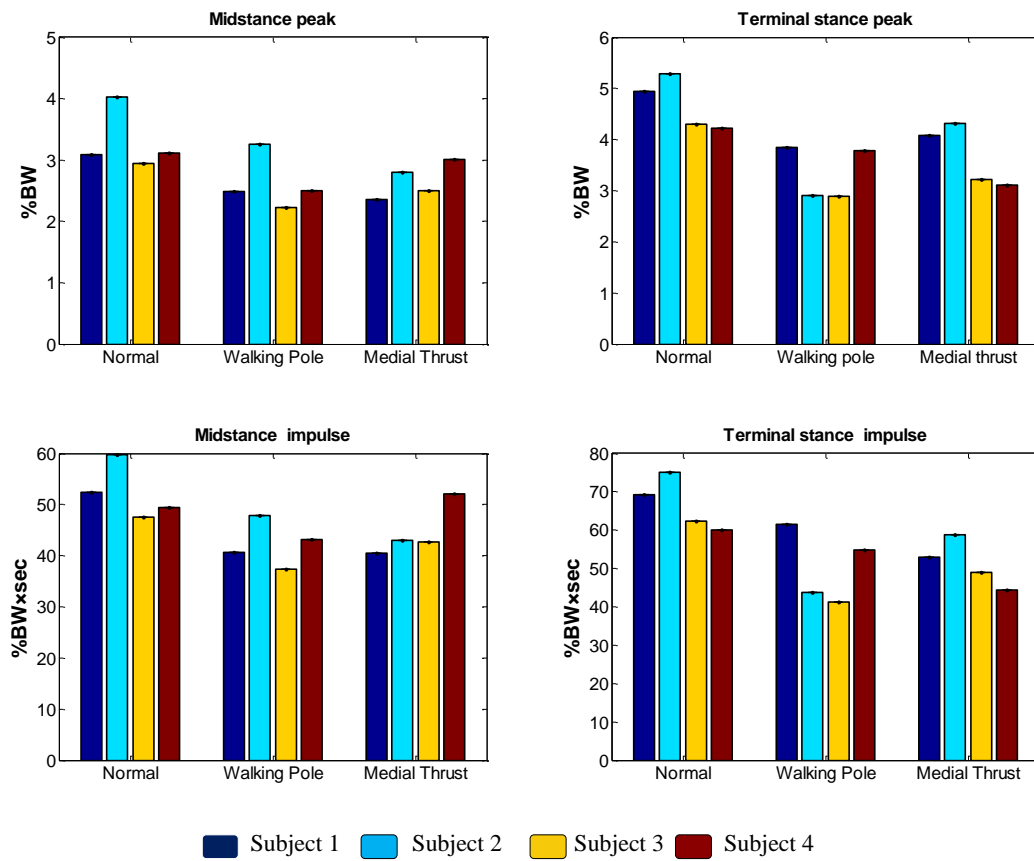


Figure 11 Both medial thrust-based kinematics and walking pole-based kinematics could decrease knee joint loadings in terms of the peak and angular impulse values in the midstance and terminal stance phases.

**Supplementary data**

[Click here to download Supplementary data: Appendix.docx](#)